Controlled Nitroxide-Mediated Styrene Surface Graft Polymerization with Atmospheric Plasma Surface Activation

Gregory T. Lewis and Yoram Cohen*

Department of Chemical and Biomolecular Engineering, University of California, Los Angeles, California 90095-1592

Received February 6, 2008. Revised Manuscript Received July 15, 2008

Polymer layer growth by free radical graft polymerization (FRGP) and controlled nitroxide-mediated graft polymerization (NMGP) of polystyrene was achieved by atmospheric pressure hydrogen plasma surface activation of silicon. Kinetic polystyrene layer growth by atmospheric pressure plasma-induced FRGP (APPI-FRGP) exhibited a maximum surface-grafted layer thickness (125 Å after 20 h) at an initial monomer concentration of $[M]_0 = 2.62$ M at 85 °C. Increasing both the reaction temperature ($T = 100$ °C) and initial monomer concentration ($[M]_0 = 4.36$ M) led to an increased initial film growth rate but a reduced polymer layer thickness, due to uncontrolled thermal initiation and polymer grafting from solution. Controlled atmospheric pressure plasma-induced NMGP (APPI-NMGP), using 2,2,6,6-tetramethyl-1-piperidinyloxy (TEMPO), exhibited a linear increase in grafted polystyrene layer growth with time due to controlled surface graft polymerization as well as reduced uncontrolled solution polymerization and polymer grafting, resulting in a polymer layer thickness of 285 Å after 60 h at [TEMPO] = 10 mM, $[M]_0 = 4.36$ M, and $T = 120$ °C. Atomic force microscopy (AFM) surface analysis demonstrated that polystyrene-grafted surfaces created by APPI-NMGP exhibited a high surface density of spatially homogeneous polymer features with a low root-mean-square (RMS) surface roughness ($R_{rms} = 0.36$ nm), similar to that of the native silicon surface ($R_{rms} = 0.21$ nm). In contrast, polymer films created by APPI-FRGP at $[M]_0 = 2.62$ M demonstrated an increase in polymer film surface roughness observed at reaction temperatures of 85 °C ($R_{rms} = 0.55$ nm) and 100 °C ($R_{rms} = 1.70$ nm). The present study concluded that the current approach to APPI controlled radical polymerization may be used to achieve a grafted polymer layer with a lower surface roughness and a higher fractional coverage of surface-grafted polymers compared to both conventional FRGP and APPI-FRGP.

Introduction

Surface modification of inorganic and organic materials with chemically end-grafted brush polymers combines the thermal and mechanical properties of the support material with a highly stable, functionalized polymer phase that can be tailored with unique chemical and physical properties. Structuring surfaces with end-grafted brush polymers is commonly achieved by free radical graft polymerization (FRGP), where the polymer chain size, chain length uniformity, and surface density are dictated by the initial monomer concentration, reaction temperature, and density of the surface immobilized initiators[1,2] or initiators in solution.[3−5] However, traditional FRGP results in a broad molecular weight chain size distribution, and the achievable polymer surface graft density is generally limited by activation methods that rely on initiator surfaces.[6]

Plasma-induced graft polymerization resolves the above limitations via surface activation by plasma treatment to create a dense coverage of surface-activated sites, from which liquid-phase vinyl monomer addition may proceed to form grafted polymer chains. Low pressure plasma-induced graft polymerization of polystyrene has been demonstrated for surface structuring of Nafion fuel cells,[7,8] poly(vinylidene fluoride) pervaporation membranes,[9,10] and titanium dioxide particles.[11,12] However, low pressure plasma-induced graft polymerization requires the use of vacuum chambers, which limits the practical scale-up potential for industrial applications. Recently, atmospheric pressure (AP) plasma-induced graft polymerization was used to create dense layers of end-grafted poly(vinylpyrrolidone) from inorganic silicon surfaces.[13] The surface number density of AP plasma-activated surface sites, as noted in the above study, was dependent on the adsorbed surface water coverage, which assisted in plasma surface activation, and the plasma operating parameters (i.e., surface treatment time and radio frequency power).[13−15] The resulting polymer-grafted silicon substrates were characterized by a high surface density of grafted polymer chains with a maximum polymer feature size (i.e., layer thickness) of 50−80 Å and chain spacing (i.e., surface density) of 10−50 Å, both of which scaled with initial monomer concentration.[13]

Controlled radical polymerization (CRP) has received considerable attention in recent years for enabling surface structuring. Grafted polymer domains are created via controlled polymer

* To whom correspondence should be addressed. E-mail: yoram@ucla.edu. Telephone: +(310) 825-8766. Fax: (310) 206-4107.

(1) Hyun, J.; Chilkoti, A. *Macromolecules* **2001**, *34*(16), 5644–5652.
(2) Teare, D. O. H.; Schofield, W. C. E.; Roucoules, V.; Badyal, J. P. S. *Langmuir* **2003**, *19*(6), 2398–2403.
(3) Bismarck, A.; Pfaffernoschke, M.; Springer, J.; Schulz, E. *J. Thermoplast. Compos. Mater.* **2005**, *18*(4), 307–331.
(4) Coiai, S.; Passaglia, E.; Ciardelli, F.; Tirelli, D.; Peruzzotti, F.; Resmini, E. *Macromol. Symp.* **2006**, *234*, 193–202.
(5) Hosseini, S. H. *J. Appl. Polym. Sci.* **2006**, *101*(6), 3920–3926.
(6) Yoshida, W.; Castro, R. P.; Jou, J. D.; Cohen, Y. *Langmuir* **2001**, *17*(19), 5882–5888.
(7) Bae, B.; Ha, H. Y.; Kim, D. *J. Membr. Sci.* **2006**, *276*(1−2), 51–58.
(8) Bae, B.; Kim, D. *J. Membr. Sci.* **2003**, *220*(1−2), 75–87.
(9) Ihm, C. D.; Ihm, S. K. *J. Membr. Sci.* **1995**, *98*(1−2), 89–96.
(10) Motornov, M.; Minko, S.; Eichhorn, K. J.; Nitschke, M.; Simon, F.; Stamm, M. *Langmuir* **2003**, *19*(19), 8077–8085.
(11) Zhong, S. F.; Meng, Y. D.; Ou, Q. R.; Shu, X. S. *Plasma Sci. Technol.* **2006**, *8*(3), 321–324.
(12) Zhong, S. F.; Meng, Y. D.; Ou, Q. R.; Shu, X. S. *J. Appl. Polym. Sci.* **2005**, *97*(5), 2112–2117.
(13) Lewis, G. T.; Nowling, G. R.; Hicks, R. F.; Cohen, Y. *Langmuir* **2007**, *23*(21), 10756–10764.
(14) Lu, W. L.; Huang, C. Y.; Roan, M. L. *Surf. Coat. Technol.* **2003**, *172*(2−3), 251–261.
(15) Choi, H. S.; Kim, Y. S.; Zhang, Y.; Tang, S.; Myung, S. W.; Shin, B. C. *Surf. Coat. Technol.* **2004**, *182*(1), 55–64.

10.1021/la8014173 CCC: $40.75
Published on Web 10/21/2008

chain growth and grafted chain polydispersity.[16−25] CRP utilizes a chemical agent which reversibly binds to the surface-bound macroradical chain, establishing a thermodynamic equilibrium that favors the capped polymer in the dormant phase.[26] The presence of the chemical agent limits the number of "living" chains in solution, thus enabling control over the rate of surface polymerization while reducing chain termination. Controlled polystyrene graft polymerization, with number-average molecular weights (M_n) and polydispersity indices (PDI), has been reported for the following CRP methods: atom transfer radical graft polymerization (ATRGP) (M_n = 10 400−18 000 g/mol and PDI = 1.05−1.23),[16−18,27−31] reversible addition-fragmentation chain transfer (RAFT) graft polymerization (M_n = 12 800−20 000 g/mol, PDI = 1.10−1.40),[19−21,32−34] and nitroxide-mediated graft polymerization (NMGP) (M_n = 20 000−32 000 g/mol, PDI = 1.20−1.30)[22,24,25,35−40] for grafting of polystyrene onto silica and polymeric materials (e.g., polyglycidyl methacrylate (PGMA), polythiophene, polypropylene, and polyacrylate). However, it should be noted that ATRGP and RAFT graft polymerization pose unique challenges. For example, ATRGP requires a specific and precise initiator to catalyst to monomer ratio, optimal temperature/solvent conditions, and surface-bound organic halide initiators.[16−18,27−31] Similarly, synthesis of chain transfer agents, specific for each monomer system, is necessary to achieve RAFT graft polymerization.[19−21,32−34] NMGP, on the other hand, may achieve controlled radical polymerization using commercial chemical agents (e.g., alkoxyamines) which reversibly bind to polymer chain radicals in solution and at the surface.[22,24,25,35−40]

The present study focuses on evaluating the benefit of integrating atmospheric pressure (AP) hydrogen plasma surface activation with controlled NMGP for the synthesis of nanostructured polystyrene−silicon surfaces. The rationale for the present approach is to enable the formation of a uniform and highly dense grafted polymer phase by controlled chain growth. The growth of the grafted polymer layer was analyzed, based on simple reaction schemes, to demonstrate the capability for controlled surface graft polymerization. Surface topography was characterized by atomic force microscopy (AFM) to evaluate the polymer feature height distribution and uniformity of grafted polymer surface coverage.

Materials and Methods

Materials. Prime-grade silicon ⟨100⟩ wafers used in this study were obtained from Wafernet, Inc. (San Jose, CA). Native wafer samples were single-side polished and cut to 1 cm square pieces for processing. Deionized (DI) water was produced using a Millipore (Bedford, MA) Milli-Q filtration system. Hydrofluoric acid, sulfuric acid, and aqueous hydrogen peroxide (30 vol %) were obtained from Fisher Scientific (Tustin, CA). Chlorobenzene (99%) and tetrahydrofuran (99.99%) were obtained from Fisher Scientific (Tustin, CA). Styrene (99%) with catechol inhibitor (<0.1%), obtained from Sigma Aldrich (St. Louis, MO), was purified by column chromatography using a silica column (Fisher Scientific, Tustin, CA). 2,2,6,6-Tetramethyl-1-piperidinyloxy radical (TEMPO, 98%), used as a control agent for controlled nitroxide-mediated graft polymerization, was obtained from Sigma Aldrich (St. Louis, MO) and was used as received.

Substrate Cleaning and Conditioning. Silicon wafers were cleaned (to remove adsorbed organics and the native oxide layer) by a sequential acid-etching process.[13] Briefly, the silicon substrates were cleaned in a piranha solution (70% sulfuric acid, 30% hydrogen peroxide) for 10 min at 90 °C and then triple rinsed to remove residuals. (**Caution!** *Piranha solution reacts violently with many organic materials and should be handled with extreme care.*) Substrates were then dipped in a 50 vol % aqueous solution of hydrofluoric acid to remove the native oxide layer and then triple rinsed and vacuum-dried at 100 °C. It was previously shown that the surface density of polymer anchoring sites could be maximized by optimal control of adsorbed surface water coverage.[13] Accordingly, dried silicon substrates were subsequently placed in a humidity chamber for 12 h to allow for controlled surface water adsorption.[13] The insulated chamber was maintained at a temperature of 22 °C and was humidified with DI water at 50% relative humidity (% RH).

Plasma Surface Activation and Graft Polymerization. Silicon substrates were plasma treated under an inert nitrogen atmosphere to minimize exposure to atmospheric oxygen, which is known to react with, and destroy, surface free radicals.[13] The atmospheric pressure (AP) plasma source used in the present study was a cylindrical plasma jet, and a detailed description is available elsewhere.[41] The plasma jet was positioned about 1 cm above the substrate surface and was operated at 100−250 V with a radio frequency (RF) power of 13.56 MHz. A mixture of 1 vol % ultrahigh purity hydrogen (99.999%) in helium (99.999%) was delivered to the AP plasma source at a total flow rate of about 30 L/min. Silicon substrates were plasma treated for a period of 10 s at a RF power of 40 W and then were briefly immersed in DI water.[13] For FRGP, the hydrogen plasma treated silicon substrates were graft polymerized in a 0.87−4.36 M (10−50 vol %) styrene−chlorobenzene mixture at T = 70, 85, and 100 °C. For NMGP, the hydrogen plasma treated silicon substrates were graft polymerized in a 4.36 M (50 vol %) styrene−chlorobenzene mixture at a temperature range of 100−130 °C and a TEMPO molar concentration range of 5−15 mM. Following

(16) Lindqvist, J.; Malmstrom, E. *J. Appl. Polym. Sci.* **2006**, *100*(5), 4155–4162.
(17) Shen, J.; Ogino, K. *Chem. Lett.* **2005**, *34*(12), 1616–1617.
(18) Liu, Y.; Klep, V.; Zdyrko, B.; Luzinov, I. *Langmuir* **2004**, *20*(16), 6710–6718.
(19) Wang, W. C.; Neoh, K. G.; Kang, E. T. *Macromol. Rapid Commun.* **2006**, *27*(19), 1665–1669.
(20) Roy, D.; Guthrie, J. T.; Perrier, S. *Macromolecules* **2005**, *38*(25), 10363–10372.
(21) Barner, L.; Zwaneveld, N.; Perera, S.; Pham, Y.; Davis, T. P. *J. Polym. Sci., Part A: Polym. Chem.* **2002**, *40*(23), 4180–4192.
(22) Voccia, S.; Jerome, C.; Detrembleur, C.; Leclere, P.; Gouttebaron, R.; Hecq, M.; Gilbert, B.; Lazzaroni, R.; Jerome, R. *Chem. Mater.* **2003**, *15*(4), 923–927.
(23) Han, C. H.; Butz, S.; Schmidt-Naake, G. *Angew. Makromol. Chem.* **1999**, *265*, 69–74.
(24) Miwa, Y.; Yamamoto, K.; Sakaguchi, M.; Shimada, S. *Macromolecules* **2001**, *34*(7), 2089–2094.
(25) Schulte, T.; Knoop, C. A.; Studer, A. *J. Polym. Sci., Part A: Polym. Chem.* **2004**, *42*(13), 3342–3351.
(26) Edmondson, S.; Osborne, V. L.; Huck, W. T. S. *Chem. Soc. Rev.* **2004**, *33*(1), 14–22.
(27) Kaneyoshi, H.; Matyjaszewski, K. *J. Polym. Sci., Part A: Polym. Chem.* **2007**, *45*(3), 447–459.
(28) Fonagy, T.; Schulze, U.; Komber, H.; Voigt, D.; Pionteck, J.; Bela, I. *Macromolecules* **2007**, *40*(5), 1401–1407.
(29) Sauguet, L.; Boyer, C.; Ameduri, B.; Boutevin, B. *Macromolecules* **2006**, *39*(26), 9087–9101.
(30) Save, M.; Granvorka, G.; Bernard, J.; Charleux, B.; Boissiere, C.; Grosso, D.; Sanchez, C. *Macromol. Rapid Commun.* **2006**, *27*(6), 393–398.
(31) Samadi, A.; Husson, S. M.; Liu, Y.; Luzinov, I.; Kilbey, S. M. *Macromol. Rapid Commun.* **2005**, *26*(23), 1829–1834.
(32) Patton, D. L.; Advincula, R. C. *Macromolecules* **2006**, *39*(25), 8674–8683.
(33) Rowe-Konopacki, M. D.; Boyes, S. G. *Macromolecules* **2007**, *40*(4), 879–888.
(34) Li, C.; Han, J.; Ryu, C. Y.; Benicewicz, B. C. *Macromolecules* **2006**, *39*(9), 3175–3183.
(35) Bian, K. J.; Cunningham, M. F. *J. Polym. Sci., Part A: Polym. Chem.* **2005**, *43*(10), 2145–2154.
(36) Bartholome, C.; Beyou, E.; Bourgeat-Lami, E.; Chaumont, P.; Zydowicz, N. *Polymer* **2005**, *46*(19), 8502–8510.
(37) Bartholome, C.; Beyou, E.; Bourgeat-Lami, E.; Chaumont, P.; Zydowicz, N. *Macromolecules* **2003**, *36*(21), 7946–7952.
(38) Zhao, X. D.; Fan, X. H.; Chen, X. F.; Chai, C. P.; Zhou, Q. F. *J. Polym. Sci., Part A: Polym. Chem.* **2006**, *44*(15), 4656–4667.
(39) Bartholome, C.; Beyou, E.; Bourgeat-Lami, E.; Chaumont, P.; Lefebvre, F.; Zydowicz, N. *Macromolecules* **2005**, *38*(4), 1099–1106.
(40) Matsuno, R.; Yamamoto, K.; Otsuka, H.; Takahara, A. *Macromolecules* **2004**, *37*(6), 2203–2209.
(41) Schutze, A.; Jeong, J. Y.; Babayan, S. E.; Park, J.; Selwyn, G. S.; Hicks, R. F. *IEEE Trans. Plasma Sci.* **1998**, *26*(6), 1685–1694.

the polymerization reaction, the polymer modified silicon substrates, for both FRGP and NMGP, were sonicated for 2 h in toluene at room temperature to remove surface adsorbed homopolymers, rinsed in tetrahydrofuran, and vacuum-dried at 100 °C.

Surface Characterization. Surface modification of the silicon surfaces was confirmed by attenuated total reflectance Fourier transform infrared (ATR-FTIR) spectroscopy using a BioRad FTS-40 FTIR instrument equipped with an attenuated total reflectance accessory (BioRad Digilab Division, Cambridge, MA). ATR-FTIR spectra for polystyrene-grafted substrates were post-processed, and all spectra were reported in terms of Kubelka−Munk absorbance units.[42]

The grafted polystyrene layer thickness was determined using a Sopra GES5 spectroscopic ellipsometer (SE) (Westford, MA). The broadband variable angle SE was operated over the range of 250−850 nm, and the data were analyzed using multilayer polymer film models that were fitted using the nonlinear Levenberg−Marquardt regression algorithm to extract the polystyrene layer thickness. Each reported measurement was averaged over five locations on the substrate, and the resulting standard deviation for all the surfaces did not exceed 10% of the measured layer thickness.

Contact angle measurements for the polystyrene-grafted silicon substrates were determined by the sessile-drop method with a Kruss model G-23 contact angle instrument (Hamburg, Germany).[43] Before the measurements, each substrate was rinsed and sonicated separately in tetrahydrofuran and then water followed by vacuum drying at 80 °C. Contact angle measurements were made using DI water at 22 °C and about 30% RH. Each reported contact angle datum was obtained by averaging the results from at least five separate (but of identical size) drops on different areas of the given substrate.

Atomic force microscopy (AFM) surface analysis was used to measure the surface feature height distribution (i.e., the *Z*-height of the polymer features from the surface), surface roughness, feature diameter, and surface coverage of the polystyrene modified surfaces. Tapping mode AFM analysis was performed using a Multimode atomic force microscope with a Nanoscope IIIa SPM controller (Digital Instruments, Santa Barbara, CA) using NSC15 silicon nitride probes (Digital Instruments, Veeco Metrology Group, Santa Barbara, CA). AFM scans of $1 \times 1\ \mu m^2$ substrate areas were taken, at a scan rate of 0.5−1.0 Hz, at five different locations for each substrate sample, with two scans taken for each location. Surfaces were imaged at 0° and 90° to verify that images were free of directional distortions.

The root-mean-square (RMS) surface roughness, R_{rms}, was calculated from the height data and determined from

$$R_{RMS} = \sqrt{\frac{\sum (Z_i - Z_{avg})^2}{N}} \quad (1)$$

where Z_i is the ith height sample out of N total samples and Z_{avg} is the mean height. The skewness, S_{skew}, which is a measure of the asymmetry of the height distribution data about the mean, was determined from

$$S_{skew} = \frac{\sum (Z_i - Z_{avg})^3}{(N-1)\sigma^3} \quad (2)$$

where σ is the standard deviation. In order to provide a measure of the grafted polymer feature height distribution relative to the native substrate, the average *Z*-height of the native silicon surface (0.3−0.5 nm), determined from five locations for each surface, was subtracted from the surface feature height data for the polymer modified substrate. The adjusted *Z*-height data were then fitted to a Gaussian distribution to clarify the presence of tails (small or large features) in the distribution.

Graft Polymerization Schemes

Polystyrene Plasma-Induced Graft Polymerization Scheme. The characteristics of the graft polymerized layer (e.g., topography, surface uniformity, and surface feature density) were affected by the reaction conditions, which could in turn be adjusted to synthesize the desired properties of the grafted polymer layer. Therefore, it is instructive to explore the potential reaction mechanisms responsible for the resulting graft polymerized polystyrene layers. Accordingly, a general reaction scheme for atmospheric pressure plasma-induced free radical graft polymerization (APPI-FRGP) and nitroxide-mediated graft polymerization (APPI-NMGP) of polystyrene is illustrated in Table 1. The proposed reaction scheme considers two initiation mechanisms: (1) AP hydrogen plasma surface activation followed by surface initiation (eq 3a−f) and (2) thermal solution initiation (eq 4a−d) of styrene monomer, which for styrene polymerization is significant at reaction temperatures of approximately $T \geq 100$ °C.[44−46] Plasma surface activation is achieved by the dissociation of molecular hydrogen in gas phase collisions to form hydrogen plasma (eq 3a) which may react with surface sites and adsorbed surface water (eq 3c) to form surface-activated sites (SI).[47] The plasma-activated surface sites have been previously characterized as surface peroxides by FTIR spectroscopy and a surface radical binding assay.[13] Activated sites may be destroyed when the surface is sufficiently oversaturated by plasma species (eq 3d).[13] However, precise control of the plasma treatment time and RF power limits surface passivation and allows for a highly dense surface coverage of radical initiators (eq 3e), from which vinyl monomers may combine to form surface-grafted polymer chains (S_n•) (eq 3f, where S designates a surface anchoring site and n is the number of monomers in the surface anchored chain). At elevated temperatures, thermal solution initiation may occur, whereby monomer decomposition leads to the formation of a Diels−Alder adduct (AH) from styrene (eq 4a), followed by molecular homolysis of AH and styrene (eq 4b),[48,49] to form radical initiators in solution (eq 4c,d) which may combine with surface growing chains (eq 7e,f) and initiate the growth of polymer chains in solution. Once polymer chain growth (in solution or on the surface) is initiated, the chains continue to grow by monomer propagation (eq 5a,c) with chain growth impacted by chain transfer (eq 6a,b) and chain termination (eq 7a−f).[50] Controlled polymer growth at the surface and in solution by NMGP may be attained by reversible coupling with TEMPO (T, eq 5b,d) to yield polymers with narrower size distributions than possible by FRGP.

Plasma-Induced FRGP Scheme. Surface graft polymerization by monomer addition from plasma-activated surface sites would be expected to prevail when thermal initiation of monomer in solution does not occur or is at a sufficiently slow rate of initiation ($\sim T \leq 100$ °C).[48,49] At higher reaction temperatures (i.e., $T \geq 100$ °C), thermal monomer initiation in solution may be significant,[48,49] leading to the formation of bulk phase macroradicals that may react with active surface sites (eq 7e,f). Accordingly, styrene graft polymerization was evaluated in the present study for the above two graft polymerization regimes:

(42) Pere, E.; Cardy, H.; Cairon, O.; Simon, M.; Lacombe, S. *Vib. Spectrosc.* **2001**, *25*(2), 163–175.
(43) Faibish, R. S.; Yoshida, W.; Cohen, Y. *J. Colloid Interface Sci.* **2002**, *256*(2), 341–350.
(44) Pan, G. F.; Sudol, E. D.; Dimonie, V. L.; El-Aasser, M. S. *J. Polym. Sci., Part A: Polym. Chem.* **2004**, *42*(19), 4921–4932.
(45) Kotoulas, C.; Krallis, A.; Pladis, P.; Kiparissides, C. *Macromol. Chem. Phys.* **2003**, *204*(10), 1305–1314.
(46) Khuong, K. S.; Jones, W. H.; Pryor, W. A.; Houk, K. N. *J. Am. Chem. Soc.* **2005**, *127*(4), 1265–1277.
(47) Moravej, M.; Babayan, S. E.; Nowling, G. R.; Iang, X.; Hicks, R. F. *Plasma Sources Sci. Technol.* **2004**, *13*(1), 8–14.
(48) Mayo, F. R. *J. Am. Chem. Soc.* **1953**, *75*(24), 6133–6141.
(49) Mayo, F. R. *J. Am. Chem. Soc.* **1968**, *90*(5), 1289–1295.
(50) Nguyen, V.; Yoshida, W.; Jou, J. D.; Cohen, Y. *J. Polym. Sci., Part A: Polym. Chem.* **2002**, *40*(1), 26–42.

(a) regime I, for which surface chain growth is dominated by monomer addition (at 70 and 85 °C), and (b) regime II, for which macroradicals, formed by thermal initiation, may bind to the surface, affecting the growth and limiting the surface density of the graft polymer layer (at 100 °C).

The rate of monomer addition to surface chains by FRGP[50] (R_{sp}^{I}) in regime I (i.e., "grafting from", with limited thermal solution initiation) can be approximated, by using PSSH, to be the following:

$$R_{sp}^{I} = k_{sp}[S_n\bullet][M] = k_{sp}\left[\frac{f_d k_{sd}}{k_{ts}}\right]^{1/2}[SI]^{1/2}[M] \quad (8)$$

where k_{sp}, k_{sd}, and k_{ts} are the rate coefficients for surface-bound chain propagation, initiator decomposition, and polymer chain termination at the surface (i.e., by combination and disproportionation, $k_{ts} = k_{tcss}+k_{tdss}$), respectively; [$S_n$•] and [M] are the concentrations of surface-bound polymer radicals and monomer in solution, respectively; and [SI] is the concentration of activated surface species which decompose by thermally enhanced, first-order decomposition kinetics [i.e., $[SI] = [SI]_0 \exp(-fk_{sd}t)$].[50−52] Thermal first-order decomposition of surface peroxides has been previously demonstrated for surface activation by gamma irradiation[53] and UV irradiation.[54]

The rate of monomer consumption (or polymerization) in regime II, R_m^{II}, can be approximated as the sum of the rate of surface graft polymerization, R_{sp}^{I}, and the rate of polymerization in solution due to thermal initiation, R_{pp}^{T} (i.e., $R_m^{II} = R_{sp}^{I} + R_{pp}^{T} = k_{sp}[S_n\bullet][M] + k_{pp}[P_n\bullet][M]$), if one assumes that the fraction of monomer consumed in the chain transfer and termination reactions is negligible compared to monomer addition. The concentration of macroradical chains formed in solution ([P_n•]) by thermal solution initiation may be derived from the Mayo mechanism[48,49] and is expressed as the following:

$$[P_n\bullet] = \left(\frac{(k_{tsam} + k_{tsmm})[M\bullet][M]}{2(k_{tcpp} + k_{tdpp})}\right)^{1/2} \quad (9)$$

where k_{tsam} and k_{tsmm} are the rate constants for thermal solution initiation by the Diels−Alder adduct and monomer decomposition; k_{tcpp} and k_{tdpp} are the rate constants for chain combination and disproportionation in solution; and [M•] is the concentration of monomer radicals in solution ($[M\bullet] = 2k_{tsai}[M]/(k_{tsam}+k_{tsmm})$, where k_{tsai} is the rate constant for initiation by the Diels−Alder adduct.[48,49]) It should be noted, however, that the rate of polymer film growth in regime II (R_{sp}^{II}) is the combination of the rate of surface graft polymerization (R_{sp}^{I}) and the rate of polymer grafting of chains, thermally initiated in solution, to surface growing chains (S_n•) and surface-activated sites (S•), given by the following expression: $R_{sp}^{II} = R_{sp}^{I} + k'[P_n\bullet]([S_n\bullet]+[S\bullet])$, where k' is the rate constant for polymer grafting. Then, as the rate of thermal solution initiation increases with reaction temperature, the formation of macroradical chains leads to increased polymer grafting (i.e., "grafting to") of P_n• chains to the surface (eq 7e).

Plasma-Induced NMGP. Nitroxide-mediated graft polymerization (NMGP) from plasma-activated surface sites is achieved when a chemical agent (i.e., TEMPO) reversibly binds to growing (or "living") surface-bound polymer chains. Due to the fast exchange of the TEMPO radicals with the polymer chains, a quasi-equilibrium is established and the concentration of dormant and growing chains at the surface and in solution can be expressed as follows:[44,55]

$$k_{deact}[S_n\bullet]^*[T]^* = k_{act}[S_n - T]^* \quad (10)$$

$$k_{deact}[P_n\bullet]^*[T]^* = k_{act}[P_n - T]^* \quad (11)$$

where k_{deact} and k_{act} are the deactivation and activation rate constants for the controlled polymerization reaction, respectively; [T], [S_n − T], and [P_n − T] are the concentrations of TEMPO and TEMPO-bound polymers at the surface and in solution, respectively; and the superscript * denotes species that are present in solution at steady-state concentrations. The concentration of chains growing from the surface ([S_n•]) may be written, from eq 10, in the following form:

$$[S_n\bullet] = \frac{k_{act}}{k_{deact}}\frac{[S_n - T]^*}{[T]^*} = K\frac{[S_n - T]^*}{[T]^*} \quad (12)$$

where K is the activation−deactivation equilibrium constant. The rate of nitroxide-mediated surface polymerization is obtained by the combination of eqs 8 and 12 to give the following expression:

$$R_{sp} = K_{app}[M] \quad (13)$$

where $K_{app} = k_{sp}K[S_n - T]^*/[T]^*$ is the apparent equilibrium rate coefficient.

Results and Discussion

Polystyrene was chemically grafted to silicon using a two-step plasma-induced graft polymerization approach combining surface activation by atmospheric pressure (AP) plasma surface treatment with styrene graft polymerization by monomer addition to activated surface sites (Table 1). Consistent with previous work,[13] the surface density of surface initiation sites and grafted polymer chains was dependent on the plasma processing parameters (i.e., surface conditioning, plasma treatment time, and RF power). The reaction conditions, specifically the initial monomer concentration and temperature, determined the surface-bound polymer chain properties (i.e., polymer layer thickness), which may be concluded from the established reaction mechanism for FRGP.[50] Energy dispersive spectroscopy (EDS) analysis of the polystyrene modified surface confirmed the presence of carbon atoms at the substrate, corresponding to the polymer carbon chain structure and styrene functional groups. ATR-FTIR surface analysis (Figure 1) of the modified silicon substrate revealed Si−O bond bending and stretching (between 1900−2200 and 700−1000 cm^{-1}) as a result of plasma surface treatment and Si−H bond stretching (near 1200 cm^{-1}) corresponding to the native silicon. Grafted polystyrene was identified in the IR spectrum with peaks identifying the alkane C−C and alkene C=C bond stretching (at 3000 cm^{-1}), which corresponded to the benzene functional groups.

Atmospheric Pressure Plasma-Induced FRGP (APPI-FRGP) Layer Growth. In order to determine the plasma-induced FRGP reaction conditions to maximize the polystyrene film thickness, a series of graft polymerization experiments were carried out (up to a reaction time of 8 h) at an initial styrene concentration range of 0.87−4.36 M (10−50 vol %) at 85 °C (Figure 2). An increase in polymer layer thickness with initial monomer concentration was observed from $[M]_0 = 0.87$ to 2.62 M, with a maximum polystyrene film thickness of 75 Å at $[M]_0 = 2.62$ M. The grafted polymer layer thickness formed at $[M]_0 = 2.62$ M was about a factor of 5 higher than that at $[M]_0 = 0.87$ M (15 Å). However, upon increasing the initial monomer concentration to $[M]_0 = 4.36$ M, only a 55 Å grafted polystyrene layer thickness could be achieved, more than a 25% reduction relative to $[M]_0 = 2.62$ M. The increase in grafted polymer layer

Table 1. Proposed Reaction Scheme for Plasma-Induced Free Radical Graft Polymerization (APPI-FRGP: eqs 5a,c) and Controlled Nitroxide-Mediated Graft Polymerization (APPI-NMGP: eqs 5b,d) of Polystyrene on Silicon

Plasma Activation and Surface Initiation

$$H_2 + e^- \xrightarrow{k_{hdis}} H + H + e^- \quad (3a)$$

$$H + H + He \xrightarrow{k_{hcomb}} H_2 + He \quad (3b)$$

$$H + S + H_2O \xrightarrow{k_{si}} SI \quad (3c)$$

$$SI + H \xrightarrow{k_{st}} S \quad (3d)$$

$$SI \xrightarrow{k_{sd}} S\bullet \quad (3e)$$

$$S\bullet + M \xrightarrow{k_{mi}} S_n\bullet \quad (3f)$$

Thermal Solution Initiation

$$2M \xrightarrow{k_{tsmi}} AH \quad (4a)$$

$$AH + M \xrightarrow{k_{tsai}} A\bullet + M\bullet \quad (4b)$$

$$A\bullet + M \xrightarrow{k_{tsam}} P_n\bullet \quad (4c)$$

$$M\bullet + M \xrightarrow{k_{tsmm}} P_n\bullet \quad (4d)$$

Propagation

$$S_n\bullet + M \xrightarrow{k_{sp}} S_{n+1}\bullet \quad (5a)$$

$$S_n\bullet + T \underset{k_{act}}{\overset{k_{deact}}{\rightleftharpoons}} S_n - T \quad (5b)$$

$$P_n\bullet + M \xrightarrow{k_{pp}} P_{n+1}\bullet \quad (5c)$$

$$P_n\bullet + T \underset{k_{act}}{\overset{k_{deact}}{\rightleftharpoons}} P_n - T \quad (5d)$$

Chain Transfer

$$S_n\bullet + M \xrightarrow{k_{trs}} S_n + M\bullet \quad (6a)$$

$$P_n\bullet + M \xrightarrow{k_{trp}} P_n + M\bullet \quad (6b)$$

Termination

$$S_n\bullet + S_m\bullet \xrightarrow{k_{tcss}} S_n - S_m \quad (7a)$$

$$S_n\bullet + S_m\bullet \xrightarrow{k_{tdss}} S_n + S_m \quad (7b)$$

$$P_n\bullet + P_m\bullet \xrightarrow{k_{tcpp}} P_n - P_m \quad (7c)$$

$$P_n\bullet + P_m\bullet \xrightarrow{k_{tdpp}} P_n + P_m \quad (7d)$$

$$S_n\bullet + P_m\bullet \xrightarrow{k_{tcsp}} S_n - P_m \quad (7e)$$

$$S_n\bullet + P_m\bullet \xrightarrow{k_{tdsp}} S_n + P_m \quad (7f)$$

thickness with initial monomer concentration ($[M]_0 = 0.87-2.62$ M) was expected, as implied by the FRGP kinetic equation for the rate of monomer addition to surface chains (eq 8). For the range of low initial monomer concentrations, the polymer layer thickness increased with monomer concentration, suggesting that the rate of monomer addition dominated surface graft polymerization. The existence of a maximum layer thickness was not surprising, however, given the expected competition between graft polymerization (eq 5a) and chain termination (eq 7a−f). It is hypothesized that, above a critical initial monomer concentration, the rate of polymer grafting (eq 7e,f) from

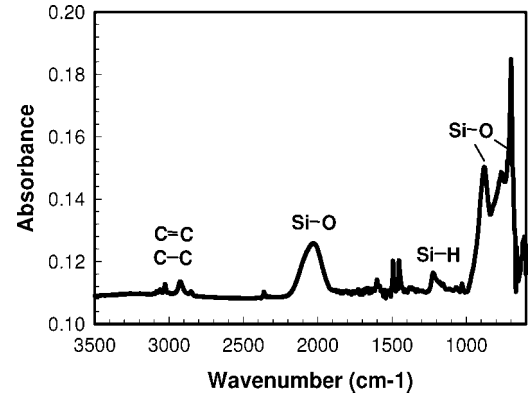

Figure 1. ATR-FTIR spectroscopy of polystyrene surface structuring of a silicon surface by atmospheric pressure plasma-induced graft polymerization.

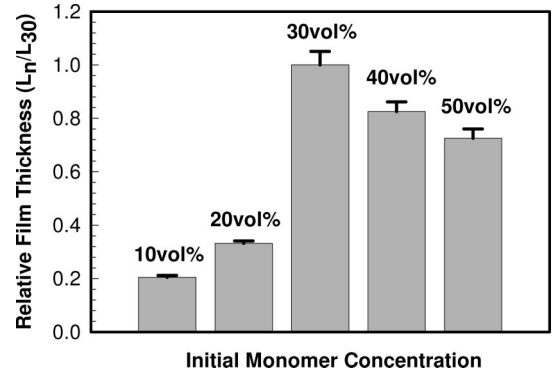

Figure 2. Relative polymer film thickness achieved by APPI-FRGP at an initial monomer concentration of $[M]_0 = 0.87-4.36$ M (10−50 vol %) at $T = 85$ °C after an 8 h reaction period (L_{30} = film thickness at 30 vol %). Plasma surface activation: treatment time = 10 s, RF power = 40 W, and RH = 50% at 22 °C.

macroradicals, which are formed by surface-initiator fragmentation and monomer addition in solution, and surface-bound chain termination (eq 7a,b) led to a reduction in the number of surface anchored macroradicals that could continue to grow by monomer propagation. As a result, chain growth diminished, noted by a reduction in grafted polymer layer thickness.

Polystyrene film growth in regime I (APPI-FRGP at 70 and 85 °C) and regime II (APPI-FRGP with thermal solution initiation at 100 °C), at the previously noted optimal reaction condition of $[M]_0 = 2.62$ M (30 vol %), exhibited strikingly different film growth behavior, with a high initial growth rate observed in regime II and a lower growth rate but somewhat more linear polymer growth observed in regime I (Figure 3a). The polymer layer growth at 100 °C was characterized by an initial growth rate of 45 Å/h at 30 min (Figure 4a) that appeared to approach a plateau with respect to time, reaching a polymer film thickness of about 80 Å after 7 h (Figure 3a). In contrast, polymer layer growth at 70 and 85 °C exhibited a lower initial growth rate with respect to time, resulting in a polymer growth rate of about 22 Å/h at 30 min for both reaction temperatures (Figure 4a) and a polymer film thickness of 125 and 42 Å after 20 h at 85 and 70 °C, respectively (Figure 3a). The increase in the initial rate of polymer film growth from regime I to regime II was expected, given the increase in k_{sp} with temperature, which has been shown to follow an Arrhenius dependence.[50] However, the observed decline in polymer growth after about 5 h in regime II may be due to polymer grafting of macroradical polymers, formed in solution by thermal initiation, to growing surface chains and

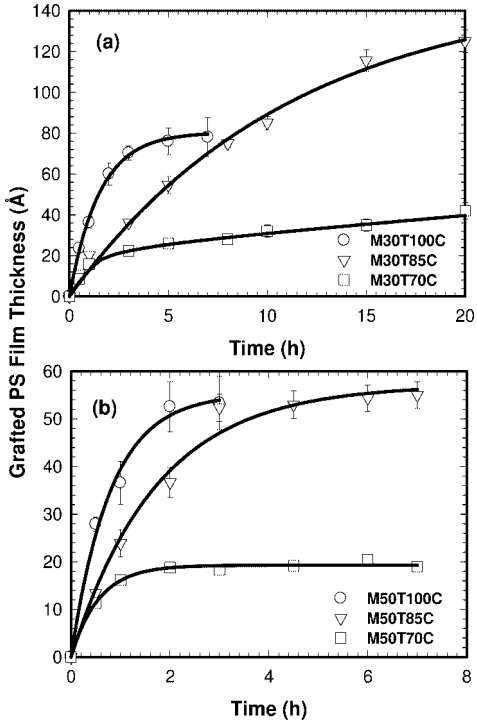

Figure 3. Polymer layer growth by APPI-FRGP at $T = 70$, 85, and 100 °C: (a) $[M]_0 = 2.62$ M, and (b) $[M]_0 = 4.36$ M. Plasma surface activation: treatment time = 10 s, RF power = 40 W, and RH = 50% at 22 °C.

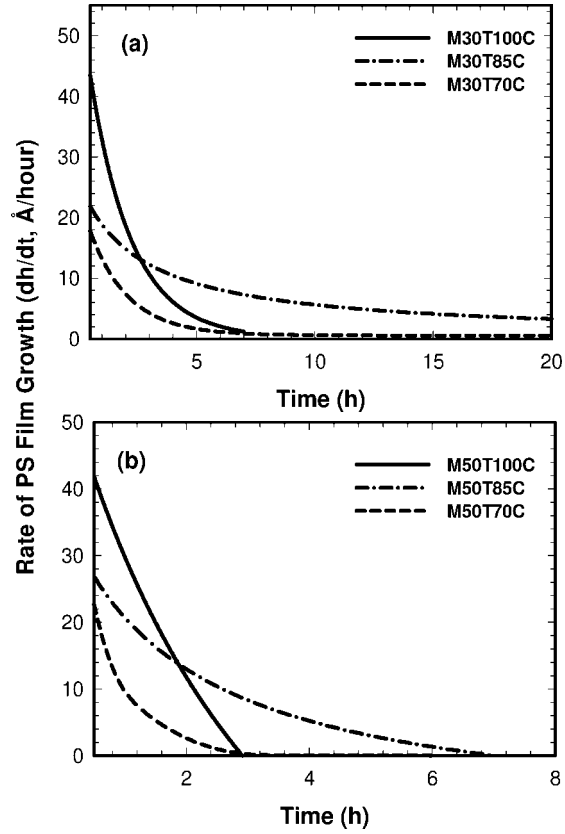

Figure 4. Film growth rate versus reaction time for APPI-FRGP at $T = 70$, 85, and 100 °C: (a) $[M]_0 = 2.62$ M, and (b) $[M]_0 = 4.36$ M. Plasma surface activation: treatment time = 10 s, RF power = 40 W, and RH = 50% at 22 °C.

thus terminating further surface chain growth (eq 7e,f). Indeed, at the higher temperature (100 °C), there was a 36% decrease in polystyrene film thickness, relative to graft polymerization at 85 °C. APPI-FRGP at 70 and 85 °C, on the other hand, appeared to exhibit a lesser deviation from linear growth behavior, presumably due to reduced thermal solution initiation and polymer grafting, and allowed for reasonable growth (via monomer addition) from surface chains. The evolution of polymer growth and polymer surface coverage was also observed by an increase in water contact angle (i.e., decreased surface wetting) with reaction time from 70 to 100 °C at $[M]_0 = 2.62$ M (Table 2). The water contact angle (CA_w) increased as the polymer layer thickness increased from regime I to regime II at $[M]_0 = 2.62$ M. For example, for APPI-FRGP at 70 °C, a 46% increase in the contact angle ($CA_w = 57.9°$) corresponded to an increase in grafted polystyrene film thickness from 8 to 32 Å after 10 h, relative to the plasma treated silicon surface ($CA_w = 39.5°$). Also, graft polymerization at 100 °C for 5 h resulted in a polystyrene film thickness of about 80 Å and a contact angle of 90°, which agreed with previous studies which reported a 90−94° water contact angle for polystyrene films on mica and silica.[56,57] Although graft polymerization at 100 °C (after 5 h), compared to 85 °C (after 10 h), resulted in a similar polymer film thickness, the water contact angle at 100 °C was about 22% greater than that at 85 °C. This increase in contact angle may be a result of the expected increase in the rate of surface initiation, and, therefore, greater surface coverage by grafted polystyrene, at higher reaction temperatures.

Table 2. Water Contact Angle Measurements (deg) of Polystyrene Layers Grafted to Silicon by APPI-FRGP and the High-Low Temperature (HLT) Graft Polymerization Sequence

	graft polymerization reaction time				
T (°C)[b]	1 h	3 h	5 h	8 h	10 h
70	49.3°	51.1°	55.7°	56.2°	57.9°
85	53.7°	59.0°	69.5°	71.6°	73.3°
100	75.7°	85.5°	90.0°	90.0°	—[a]
high-low temp[c]	76.3°	80.5°	83.0°	90.0°	90.0°

[a] Contact angle not measured. [b] Initial monomer concentration of $[M]_0 = 2.62$ M. [c] High-low temperature graft polymerization: step 1 period of 15 min at $T = 100$ °C and graft polymerization at $T = 85$ °C for the remaining reaction period.

The initial rate of polystyrene film growth was higher when the initial monomer concentration increased from 2.62 M (30 vol %) to 4.36 M (50 vol %) for reaction conditions at 70, 85, and 100 °C (Figure 3b). Over the first 30 min, the film growth rate at $[M]_0 = 4.36$ M, compared to $[M]_0 = 2.62$ M, increased by more than 10% and 20% at 70 and 85 °C, respectively (Figure 4b). However, it was noted that the polymer layer growth approached a plateau within a shorter reaction time at the higher initial monomer concentration. The increase in the rate of polymer layer growth may be the result of a higher monomer concentration at the surface and, therefore, increased rate of monomer addition to surface-activated sites. Formation of a higher density of surface-bound polymer chains may lead to diminished polymer layer growth due to an increase in surface-bound polymer−polymer chain combination (eq 7a,b), polymer grafting of chains formed

(51) Gee, G.; Cuthbertson, A. C.; Rideal, E. K. *Proc. R. Soc. London, Ser. A* **1939**, *170*, 300.
(52) Gee, G.; Rideal, E. K. *Trans. Faraday Soc.* **1936**, *32*, 666.
(53) Oberbeck, W. F.; Mayhan, K. G.; James, W. J. *J. Appl. Polym. Sci.* **1978**, *22*(10), 2805–2816.
(54) Kosa, C.; Lukac, I.; Weiss, R. G. *Macromolecules* **2000**, *33*(11), 4015–4022.
(55) Connolly, T. J.; Scaiano, J. C. *Tetrahedron Lett.* **1997**, *38*(7), 1133–1136.
(56) Li, Y.; Pham, J. Q.; Johnston, K. P.; Green, P. F. *Langmuir* **2007**, *23*(19), 9785–9793.
(57) Liberelle, B.; Giasson, S. *Langmuir* **2007**, *23*(18), 9263–9270.

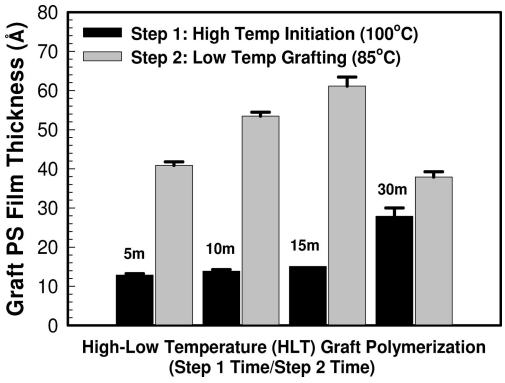

Figure 5. Film thickness achieved by the HLT APPI- FRGP sequence, illustrating the Step 1 time interval (at 100 °C) range between 5 and 30 min with a Step 2 time (at 85 °C) of 3 h. Plasma surface activation: treatment time = 10 s, RF power = 40 W, and RH = 50% at 22 °C.

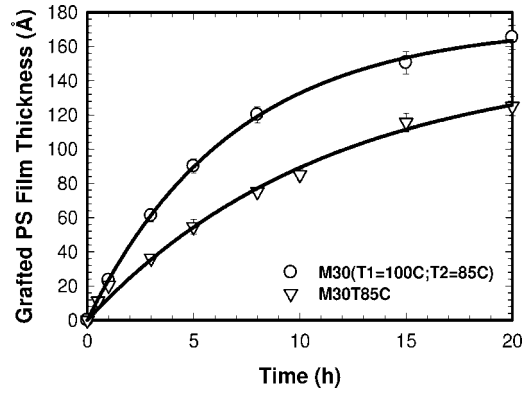

Figure 6. Polymer layer growth at $[M]_0 = 2.62$ M for the (a) HLT APPI-FRGP sequence (Step 1 = 15 min) and (b) APPI-FRGP without HLT at $T = 85$ °C. Plasma surface activation: treatment time = 10 s, RF power = 40 W, and RH = 50% at 22 °C.

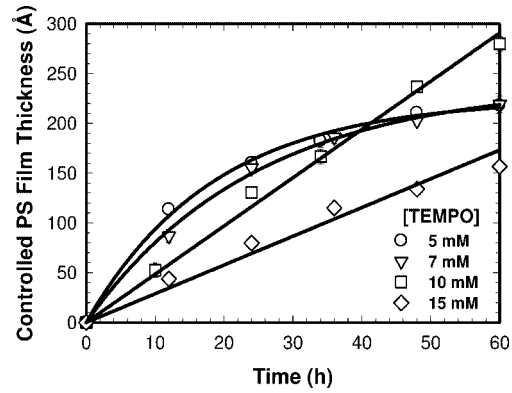

Figure 7. Polymer layer growth by controlled APPI-NMGP for $[M]_0 = 4.36$ M and [TEMPO] = 5 to 15 mM at $T = 120$ °C. Plasma surface activation: treatment time = 10 s, RF power = 40 W, and RH = 50% at 22 °C.

in solution by thermal initiation (eq 4a−d) or from initiator fragments from the surface, or chain transfer (eq 6a). Although the polystyrene film growth rate was enhanced by increasing both the initial monomer concentration and reaction temperature, the achievable film thickness and control of monomer addition to activated surface sites were reduced.

The polystyrene layer growth rate and film thickness were further improved by utilizing a High-Low Temperature (HLT) FRGP approach in which a high initial rate of polymerization was enabled ($[M]_0 = 2.62$ M) at a high temperature (Step 1, 100 °C) for a short period, followed by graft polymerization at a lower temperature (Step 2, 85 °C) to reduce the potential for polymer grafting. As shown in Figure 5, the polymer layer thickness depended on the length of the initiation step (Step 1). As the graft polymerization initiation period was increased from 5 to 15 min, the polymer layer thickness increased by more than 40% from 40 to 62 Å, respectively, after a Step 2 interval of 3 h. It is likely that the increase in Step 1 polymer layer growth was due to the higher initial rate of polymerization. A maximum in the layer thickness, achieved by the HLT FRGP sequence, was observed at 15 min. A 30% decrease in polymer layer thickness was noted when the Step 1 period was increased to 30 min, plausibly due to the formation of macroradicals by thermal solution initiation, which may have diminished polymer layer growth as the result of polymer grafting. The HLT FRGP growth behavior, for a 15 min Step 1 period, closely resembled the behavior of regime I graft polymerization at $[M]_0 = 2.62$ M and 85 °C (Figure 6). The polymer layer thickness achieved by the HLT graft polymerization sequence (165 Å after 20 h), however, was about 32% higher than that of graft polymerization at a constant temperature of 85 °C. Also, as the reaction proceeded, water contact angle measurements for the HLT prepared polymer layer reached a plateau at 90° after an 8 h reaction time, compared to 71.6° at 85 °C, suggesting a denser coverage of grafted polymer chains achieved by the rapid initiation step of the HLT approach sequence.

Atmospheric Pressure Plasma-Induced NMGP (APPI-NMGP) Layer Growth. Controlled polystyrene film growth was demonstrated by APPI-NMGP, which resulted in linear polymer layer growth with respect to time at [TEMPO] = 10 mM, $[M]_0 = 4.36$ M, and $T = 120$ °C (Figure 7). The linearity of the polystyrene film growth, with respect to time, increased with addition of the TEMPO chemical agent. Polymer layer growth for [TEMPO] = 5 and 7 mM was not controlled, as indicated by the deviation from linear film growth and reduced layer thickness (∼220 Å at 60 h). On the other hand, controlled polymer growth at [TEMPO] = 10 mM was characterized by linear film growth and a layer thickness of ∼285 Å (at 60 h). For [TEMPO] < 10 mM, the polymer layer growth behavior was similar to that achieved for FRGP, as expected when the concentration of polymer chains is much greater than that of TEMPO, leading to partially controlled radical polymerization. For example, the initial film growth rate (at 10 h) was greater at [TEMPO] = 5 mM (9.7 Å/h) and 7 mM (7.0 Å/h), compared to [TEMPO] = 10 mM (4.3 Å/h). The decrease in polymer growth rate is likely to be a consequence of the higher initial concentration of TEMPO present at the surface to reversibly cap surface-bound growing polymer chains. Therefore, a further decrease in polymer layer growth would be expected at higher TEMPO molar concentrations, as was indeed noted at [TEMPO] = 15 mM where a 3.5 Å/h film growth rate was attained.

Table 3. Polymer Film Thickness Achieved by Controlled APPI-NMGP of Polystyrene on Silicon[a]

graft polymerization conditions			
$[M]_0$ (M)	[T] (mM)	T (°C)	polymer thickness (Å)[b]
4.36	10	100	38.1 ± 6.6
4.36	10	110	53.4 ± 6.7
4.36	10	120	283.4 ± 2.2
4.36	10	130	125.2 ± 2.5

[b] Polystyrene layer thickness measured by spectroscopic ellipsometry at final data point. [a] Plasma surface activation: treatment time = 10 s, RF power = 40 W, and RH = 50% at 22°C.

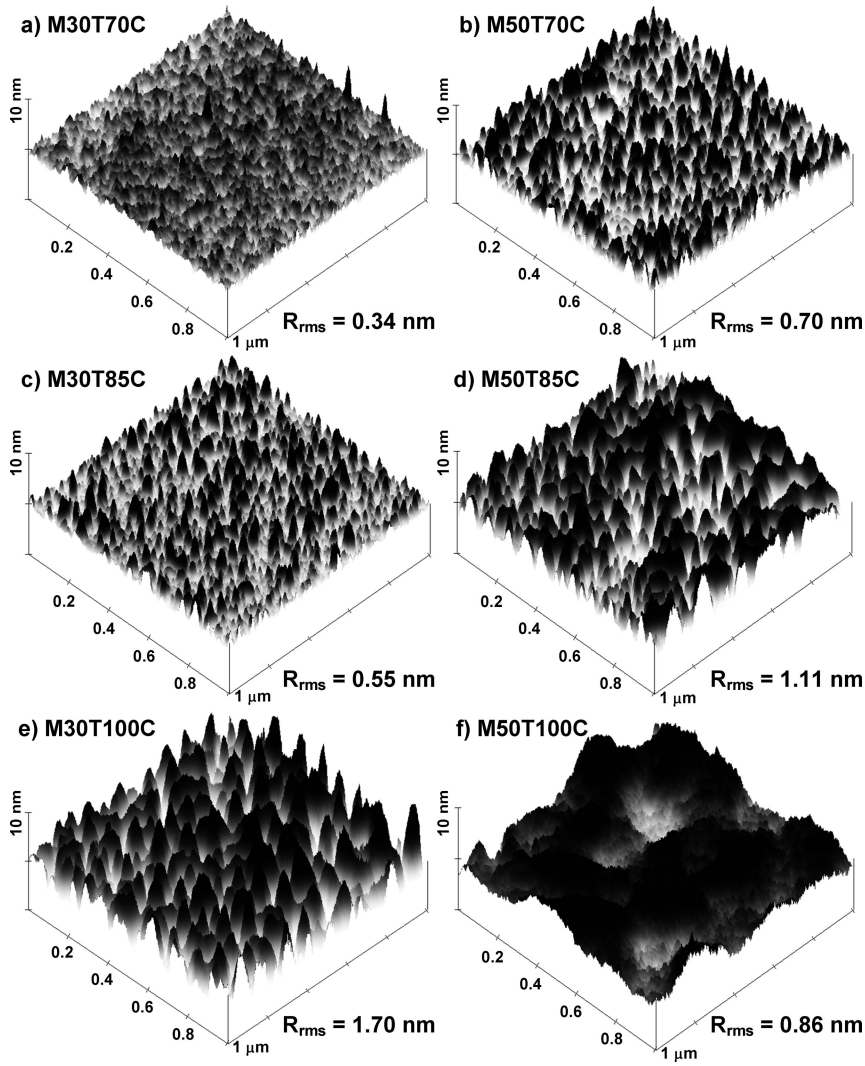

Figure 8. Tapping mode AFM surface images (1×1 μm^2) of polystyrene-grafted silicon by APPI-FRGP at $[M]_0 = 2.62$ M and (a) $T = 70$ °C, (c) $T = 85$ °C, (e) $T = 100$ °C and at $[M]_0 = 4.36$ M and (b) $T = 70$ °C, (d) $T = 85$ °C, (f) $T = 100$ °C.

The dependence of the NMGP grafted layer thickness on reaction temperature from 100 to 130 °C at [TEMPO] = 10 mM and $[M]_0 = 4.36$ M (Table 3) showed that an optimal temperature was necessary to maxmimize the polymer layer growth. The polymer film thickness by controlled APPI-NMGP, after a 60 h reaction at 100 and 110 °C, was 13% and 19%, respectively, less than the film thickness created at 120 °C. The increased rate of APPI-NMGP with temperature was consistent with work by Fukuda and co-workers[58,59] who studied the homolytic cleavage kinetics of the TEMPO−polystyrene adduct. They reported that the rate of nitroxide-mediated polymerization was 7 times greater at 120 °C, compared to 100 °C, which is in reasonable agreement with the present results of a 7.4-fold increase in polymer layer thickness (Table 3). Over the above temperature range of 120−130 °C, the polymer layer thickness decreased by more than 55% (Table 3). It is plausible that, at such a high reaction temperature (130 °C), the molar ratio of polymer macroradicals to TEMPO is much greater than unity, for both chains grown in solution and at the surface, leading to insufficient availability of TEMPO for capping chain macroradicals for controlled polymer growth. Accordingly, one would expect that when the TEMPO molar concentration is less than the total concentration of growing chains in solution and at the surface, polymer grafting (i.e., "grafting to") may be significant and thereby reduce the growth of the polymer layer.

APPI-FRGP Surface Layer Analysis. The topography (surface feature density, feature height, and feature diameter) of the polystyrene layers created by APPI-FRGP (Figures 8−10) and APPI-NMGP (Figure 11) was evaluated by AFM imaging. For polystyrene layers created by APPI-FRGP, the surface roughness and feature diameter increased with the initial monomer concentration and reaction temperature. When the initial monomer concentration was increased from $[M]_0 = 2.62$ to 4.36 M at 70 °C, the surface roughness increased dramatically from 0.34 to 0.70 nm (Figure 8a,b), with a corresponding increase in polymer feature diameters from 0−5 nm to 30−40 nm. Large grafted polymer features, formed at the high initial monomer concentration ($[M]_0 = 4.36$ M), were evidenced by the presence of a tail in the polymer feature height distribution from 2.2 to 5.0 nm (Figure 10a). Likewise, at 85 °C, an increase in surface roughness from 0.55 to 1.11 nm and average feature diameter from 15−25 to 50−60 nm was noted when the initial monomer concentration was increased from $[M]_0 = 2.62$ to 4.36M, respectively.

Similarly, when the temperature increased from 70 °C (Figure 8a) to 85 °C (Figure 8c) at $[M]_0 = 2.62$ M, the polymer feature

(58) Goto, A.; Terauchi, T.; Fukuda, T.; Miyamoto, T. *Macromol. Rapid Commun.* **1997**, *18*(8), 673–681.
(59) Fukuda, T.; Goto, A. *Macromol. Rapid Commun.* **1997**, *18*(8), 683–688.

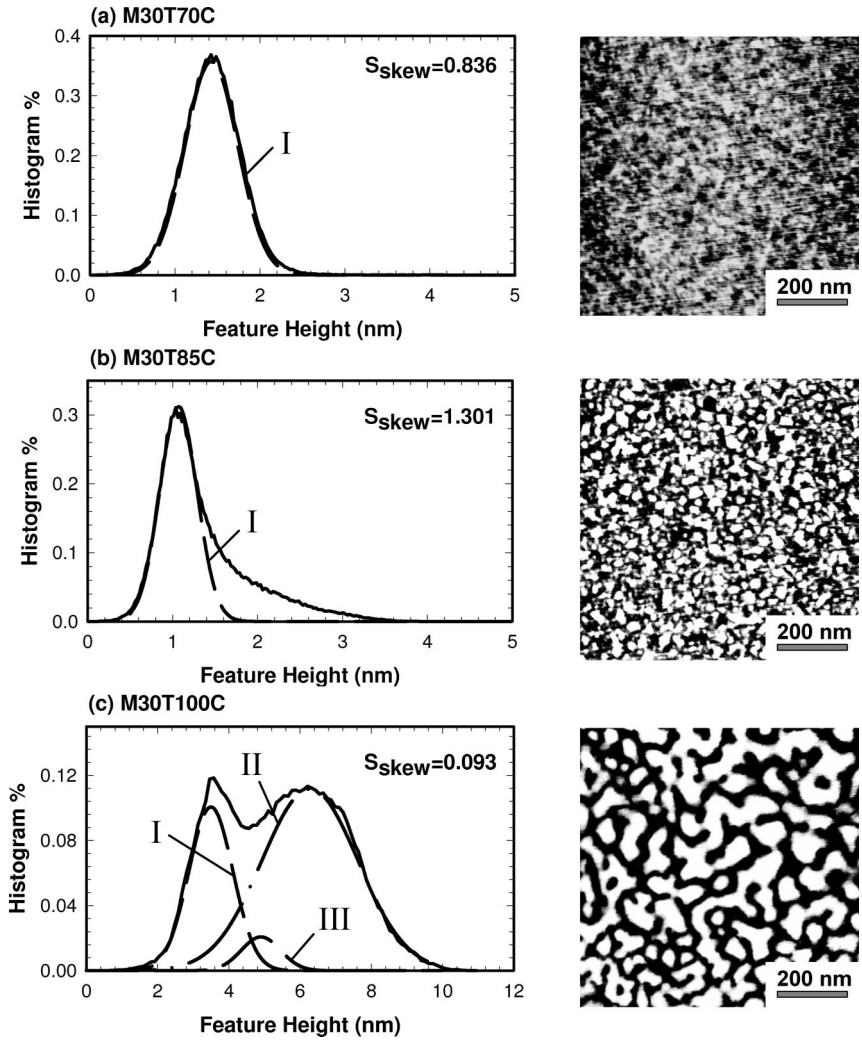

Figure 9. Polymer feature height histograms with fitted Gaussian distributions for polystyrene-grafted silicon created by APPI-FRGP at $[M]_0 = 2.62$ M and (a) $T = 70$ °C, (b) $T = 85$ °C, (c) $T = 100$ °C.

diameter range increased from 0−5 nm at 70 °C to 15−25 nm at 85 °C, and the surface roughness (R_{rms}, eq 1) increased from 0.34 nm (70 °C) to 0.55 nm (85 °C). APPI-FRGP at 100 °C (regime II) and $[M]_0 = 2.62$ M displayed the largest polymer feature diameter size of 70−90 nm (Figure 8e), with a corresponding 3-fold increase in surface roughness ($R_{rms} = 1.70$ nm), compared to APPI-FRGP at 85 °C. The contribution of polymer grafting at elevated reaction temperatures (i.e., 100 °C) to the resulting surface topography was illustrated in the bimodal surface feature height distribution (Figure 9c) that appeared to be the result of distinct but overlapping feature height distributions (I, II, and III). Feature height distribution I, which extended from about 0.5 to 5.8 nm from the surface, was considerably narrower than feature height distribution II (0.7−10.4 nm) but broader than feature height distribution III (3.2−6.6 nm). The existence of a bimodal feature height distribution suggested that uncontrolled thermal solution initiation and polymer grafting to the surface resulted in a broader range of polymer chain lengths that were grafted to the surface. Also, it is interesting to note that the feature height distribution of the polystyrene layer formed at $[M]_0 = 4.36$ M and 85 °C exhibited a similar bimodal distribution. AFM analysis illustrated that, at these conditions ($[M]_0 = 4.36$ M and 85 °C), the polystyrene layer was composed of a spatially nonuniform coverage of large globular features (Figure 8d), which may be due to polymer grafting of chains from solution, as supported by the plateau in film growth that was reached in about 6 h (Figure 3b).

Given that APPI-FRGP, at a low initial monomer concentration ($[M]_0 = 2.62$ M) and 85 °C, achieved a 3-fold increase in the film thickness (Figure 3a), relative to APPI-FRGP at 70 °C, while attaining a surface topography characterized by a low surface roughness with small surface features suggests that APPI-FRGP at 85 °C is suitable for creating a higher polymer layer thickness with relatively smooth surface features.

APPI-NMGP Surface Layer Analysis. Polystyrene-grafted silicon surfaces formed by controlled NMGP at $[M]_0 = 4.36$ M, $T = 120$ °C, and [TEMPO] = 10 mM were characterized by a spatially homogeneous, highly dense grafted polymer phase. As expected from the linear increase in film growth with respect to time (Figure 7), the grafted polymer surface appeared to be of a smooth surface topography (Figure 11b,d), evidenced by a surface roughness of 0.36 nm, nearly 80% less than that for polymer layers produced by uncontrolled APPI-FRGP in regime II at $[M]_0 = 4.36$ M ($R_{rms} = 1.70$ nm). The surface roughness and feature height distribution for the controlled polystyrene-grafted layer resembled the smooth features of the native silicon surface ($R_{rms} = 0.21$ nm). The feature height distribution (Figure 11e) illustrated a narrow polymer feature height range of about 2.4 nm with a corresponding height distribution skewness that approached zero, further demonstrating the symmetry of the

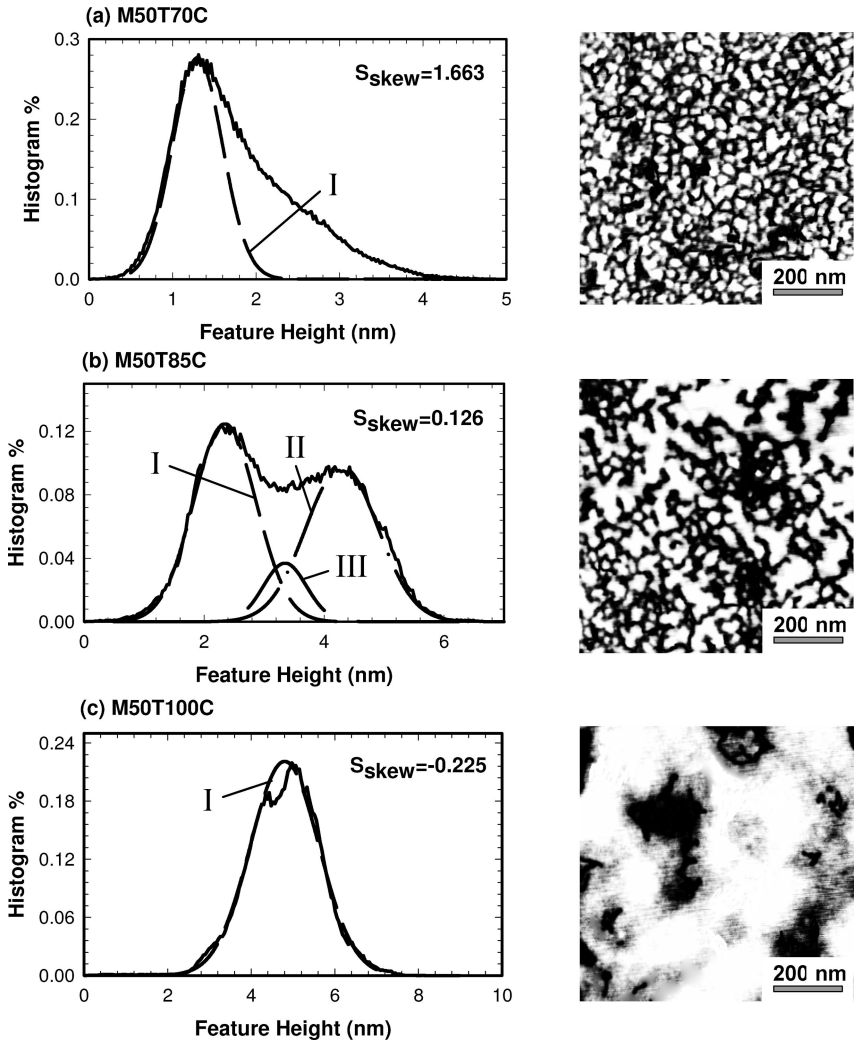

Figure 10. Polymer feature height histograms with fitted Gaussian distributions for polystyrene-grafted silicon created by APPI-FRGP at $[M]_0 =$ 4.36 M and (a) $T = 70$ °C, (b) $T = 85$ °C, (c) $T = 100$ °C.

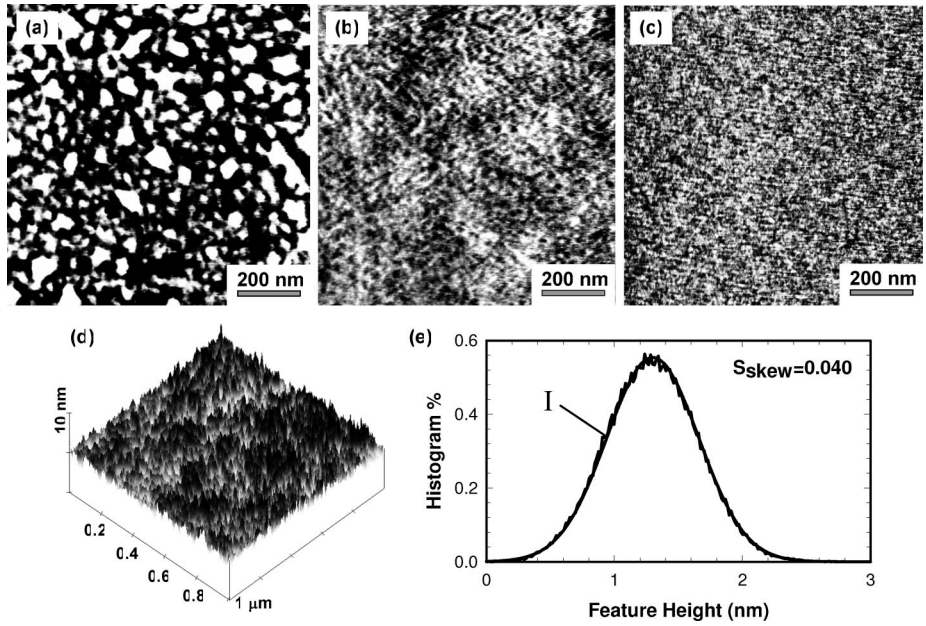

Figure 11. Tapping mode AFM images (1×1 μm^2) of polystyrene-grafted silicon by APPI-NMGP at $[M]_0 = 4.36$ M and 120 °C for [TEMPO] at (a) 5 mM, (b) 10 mM, and (c) 15 mM; (d) AFM surface image and (e) polymer feature height histogram (with fitted Gaussian distribution) at [TEMPO] = 10 mM.

feature height distribution. It should be noted that, at the lowest TEMPO molar concentration of 5 mM (Figure 11a), where less control over polymerization was attained, the formation of large polymer features was observed, similar to earlier findings for the APPI-FRGP method. Also, a comparison of APPI-NMGP at [TEMPO] = 15 mM (Figure 11c), compared to 10 mM, showed no significant change in the surface roughness and feature height distribution, as expected by the similar polymer film growth behavior at both TEMPO molar concentrations.

Conclusions

Free radical graft polymerization (FRGP) and nitroxide-mediated graft polymerization (NMGP) of polystyrene on silicon by atmospheric pressure (AP) plasma surface activation was demonstrated for a range of reaction conditions. In the absence of the TEMPO chemical agent, kinetic growth of polymer layers by APPI-FRGP demonstrated a maximum layer thickness for reaction conditions of $[M]_0 = 2.62$ M at 85 °C. An increase in the initial growth rate was noted with an increase in reaction temperature ($T = 100$ °C) and monomer concentration ($[M]_0 = 4.36$ M), due to uncontrolled thermal initiation and polymer grafting from solution. Film growth was further enhanced by a modified high-low temperature (HLT) graft polymerization sequence, whereby surface graft polymerization was conducted for a short 15 min initiation period at 100 °C followed by graft polymerization at 85 °C. The grafted film thickness attained by the above HLT graft polymerization approach was greater relative to the grafted film thickness obtained by APPI-FRGP at 85 °C. Surface grafting by controlled APPI-NMGP exhibited linear kinetic growth with respect to time, low surface roughness, and a uniform distribution of surface feature heights as measured by AFM. In contrast, AFM images of grafted polystyrene layers by APPI-FRGP illustrated highly uniform surface grafting at low monomer concentration and reaction temperature, compared to heterogeneous, globular surface feature formations that were achieved at high monomer concentration and reaction temperature.

Acknowledgment. This work was funded, in part, by the California Department of Water Resources and the U.S. Environmental Protection Agency.

LA8014173